ChemComm

Accepted Manuscript

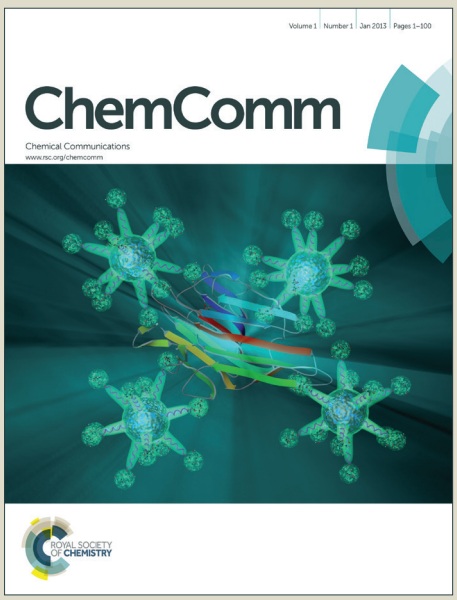

ROYAL SOCIETY OF CHEMISTRY

www.rsc.org/chemcomm

Journal Name

COMMUNICATION

Hetero-epitaxially Anchoring Au Nanoparticles onto ZnO Nanowires for CO Oxidation

Received 00th January 20xx,
Accepted 00th January 20xx

DOI: 10.1039/x0xx00000x

www.rsc.org/

Jiaxin Liu,[a,b] Botao Qiao,[a,c] Yian Song,[a] Yudong Huang[b] and Jingyue (Jimmy) Liu[a,*]

Supported Au nanoparticles (NPs) sinter easily. Anchoring Au NPs is of fundamental interest and practical importance. We stabilized Au NPs by growing them hetero-epitaxially into the facets of ZnO nanowires. The sintering of the epitaxially anchored Au NPs was significantly reduced at high calcination temperatures and during CO oxidation.

Supported metal catalysts are widely used in industry to catalyse numerous important chemical transformations. The metals are usually finely dispersed onto high-surface-area supports to maximize their atom efficiency or to tune their catalytic performances.[1] Small metal particles/clusters expose a large portion of coordinatively unsaturated atoms that render them highly reactive for specific reactions.[2] However, the high percentage of surface atoms makes the small metal particles thermodynamically unstable, especially at elevated temperatures and under catalytic reaction environments.[2-3] When supported metal nanoparticles (NPs) are used in a catalytic reaction process, their growth (sintering) can be understood in terms of two processes: Ostwald ripening (OR) or particle migration and coalescence (PMC).[4] The OR process involves inter-particle transport of mobile species driven by differences in the chemical potentials of NPs with different sizes. The final result of this OR process is the growth of larger particles at the expense of smaller ones. The PMC process, on the other hand, involves the Brownian motion of NPs or clusters, leading to coalescence when particles come in close proximity with each other.[4c-e] Therefore, smaller NPs migrate much faster than the bigger ones and the end result of the PMC process may introduce a bimodal distribution of NP sizes, and there might be denuded zones of smaller NPs immediately surrounding larger NPs. When the metal NPs are highly faceted or interact strongly with the support surface the PMC process should be significantly reduced, resulting in anchoring of metal NPs.[5] Hetero-epitaxial growth of metal NPs onto crystalline support surfaces provides an approach to enhance the metal particle-support interactions and thus the stabilization of supported metal NP catalysts.[5] We have been using this approach to develop stable, supported metal NP catalysts for various catalytic reactions.[6] Other groups have recently used similar approach to stabilize supported metal catalysts.[7] However, we communicate in this report, for the first time, the specifically designed catalyst development by hetero-epitaxial anchoring of metal NPs onto well-defined nanostructured support materials.

Oxides supported Au NPs have attracted increasing interest due to their extremely high activity and/or selectivity for numerous key chemical reactions.[8] However, a major issue for supported Au catalysts is that the Au NPs tend to sinter significantly during reaction,[9] under calcination[10] or even during storage.[11] The stability problem of supported Au catalysts has therefore become the single most critical barrier to practical applications.[12] The facile sintering behaviour of supported Au NPs may originate from their lower Tammann temperature or chemical inertness.[13] In this work, we design to anchor the Au NPs by a hetero-epitaxial growth process and thus realize the goal of stabilizing Au NPs during high temperature calcination and/or during catalytic reactions.

When all the exposed surfaces of a crystalline support possess the same surface structure and are clean then it is plausible to grow epitaxial Au NPs onto the surfaces of the support if certain conditions are met. Furthermore, the final morphology of the equilibrated Au NPs and their interfacial structure with the support surface may be similar and thus provide a nanostructured, supported metal catalyst with similar shapes of the Au NPs and interfacial structures.

To facilitate the epitaxial growth of Au NPs, ZnO nanowires (NWs), which primarily consist of flat and clean ZnO {10-10} nanoscale facets, were used to prepare the Au/ZnO catalysts. For comparison, commercially available ZnO powders were also used as support to grow the Au NPs. It was hypothesized that the majority of Au NPs would nucleate and grow epitaxially onto the clean {10-10} nanoscale facets of the ZnO NWs and that most of the Au NPs would grow onto the surfaces of the ZnO powders without specifically defined crystallographic relationships.

[a] Department of Physics, Arizona State University, Tempe, Arizona 85287, United States
[b] College of Chemical Engineering and Technology, Harbin Institute of Technology, Harbin 150001, China
[c] State Key Laboratory of Catalysis, Dalian Institute of Chemical Physics, Chinese Academy of Sciences, Dalian 116023, China

†Electronic Supplementary Information (ESI) available: Details for catalyst preparation, catalytic tests, catalyst characterization, physicochemical properties, XRD, STEM-HAADF. See DOI: 10.1039/c000000x/

The ZnO NWs were synthesized by a modified vapour transport deposition method.[14] The modified synthesis protocol can reliably be used to generate large amounts of ultrapure and high-quality ZnO NWs. The Au/ZnO-NW catalysts with a nominal 2.0 wt% loading of Au were prepared by a modified deposition-precipitation method. The precursor materials were then calcined at 200°C, 400°C and 600°C for 4 hours and the final catalysts were denoted as Au/ZnO-NW200, Au/ZnO-NW400 and Au/ZnO-NW600, respectively. Similar procedures were used to prepare Au NPs supported on ZnO powders (US Research Nanomaterials, Inc.) and these reference catalysts were denoted as Au/ZnO-P200, Au/ZnO-P400 and Au/ZnO-P600, respectively. Details of the catalyst preparation procedures, catalyst characterizations and catalytic tests were presented in the support information (SI).

The representative SEM images of the ZnO NWs and ZnO powders were presented in Fig. S1, showing the uniform morphology of the ZnO NWs and the general morphology of the ZnO powders. The total (BET) surface area of the synthesized ZnO NWs and the purchased ZnO powders are 17.61 m^2g^{-1} and 22.61 m^2g^{-1}, respectively (Table S1). Figure 1(a-c) shows the size distributions of the Au NPs in the Au/ZnO-P catalysts calcined at different temperatures. The corresponding representative high-angle annular dark-field scanning transmission electron microscopy (HAADF-STEM) images are shown in Figure S2 (a-c). The average sizes of the Au NPs in the Au/ZnO-P catalysts calcined at 200°C, 400°C and 600°C are 1.8 nm (ranging 1.0-3.0 nm), 2.8 nm (ranging 1.0-6.0 nm) and 12.8 nm (ranging 3.0-30.0 nm), respectively. These results clearly demonstrate that under calcination condition the sintering of the Au NPs in the Au/ZnO-P catalysts depends strongly on calcination temperature and that at higher calcination temperatures the sintering of the Au NPs is severe, in agreement with the results reported in literature.[15]

Figure S2 (d-f) and Figure 1(d-f) display the representative HAADF-STEM images of the Au/ZnO-NW catalysts and the corresponding size distributions of the Au NPs. The average sizes of the Au NPs in the Au/ZnO-NW catalysts, calcined at 200°C, 400°C and 600°C, are 2.4 nm (ranging 1.0-4.0 nm), 3.1 nm (ranging 1.0-6.0 nm) and 6.3 nm (ranging 3.0-12.0 nm), respectively. The slightly larger size of the Au/ZnO-NW200, compared to that of the Au/ZnO-P200, is probably due to the fact that the ZnO powders have higher total surface area and possess different facets which may interact with the small Au clusters differently. The ZnO NWs consist primarily of the low energy and stable ZnO{10-10} nanoscale facets while the ZnO powders consist of the low energy {10-10}, high energy {0001} and other high-index facets. The Au precursor materials may have interacted strongly with the various high-energy surfaces of the ZnO powders, resulting in an overall smaller Au NPs at low to moderate calcination temperatures. At higher calcination temperatures, however, the high-energy surfaces of the ZnO powders may not be stable, resulting in sintering of Au NPs. Our experimental results showed that the Au NPs sintered much slowly on the ZnO NWs than on the ZnO powders. The different sintering behaviour must have originated from the different degrees of interaction between the Au NPs and the support surfaces since both catalysts were prepared and treated via exactly the same procedures. The only difference between these two supports is the different morphologies of the ZnO crystals, which implies that the Au NPs may nucleate and grow differently on the different surfaces of the ZnO.

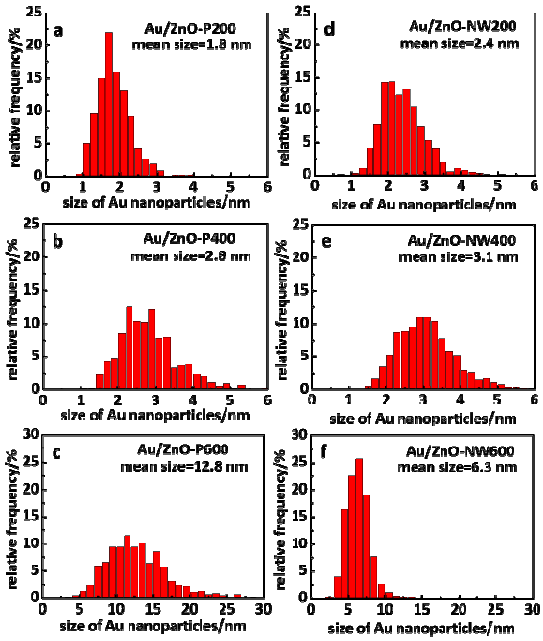

Figure 1. Size distributions of Au in (a-c) Au/ZnO-P and (d-f) Au/ZnO-NW catalysts calcined at 200°C, 400°C and 600°C, respectively.

Theoretically, the low-energy ZnO{10-10} surfaces should be stable and should not interact strongly with the Au NPs. In order to understand the Au-ZnO interactions during the calcination process sub-angstrom resolution HAADF imaging technique was used to characterize the Au/ZnO-NW system. Figure 2a shows such a representative image clearly revealing the atomic positions of the Zn and Au atoms (bright dots). The O atoms in the ZnO are not revealed in the HAADF images unless the sample is extremely thin.[5] By analysing many such images of the different regions of the Au/ZnO-NW catalysts, it was concluded that all the Au NPs grew with a fixed crystallographic orientation relationship with respect to the ZnO {10-10} nanoscale facets. From the corresponding digital diffractograms (e.g., Fig. 2b) and atomic resolution HAADF images it was deduced that the Au NPs grew with a fixed crystallographic relationship with respect to the ZnO NWs: The Au {002} planes grew parallel to the ZnO {10-11} planes, the Au {110} planes were aligned along the ZnO {11-20} planes, and the Au {111} planes form an angle of ~ 6° with respect to the ZnO {0002} planes. The epitaxial relationship can thus be designated as ZnO[11-20](1-101)//Au[110](002).

Figure 2c shows an atomic resolution HAADF image of one epitaxially anchored Au NP, clearly revealing the surface atomic arrangements of the Au NP facets. The lattice mismatch between the Au (002) planes and the ZnO (-110-1) planes is about 17.4% and the lattice mismatch between the Au (1-11) and the ZnO (0002) planes is about 9.4%. These large lattice mismatches across crystals usually do not favour epitaxial growth. By introducing interfacial dislocations, however, the domain matching epitaxy (DME) mechanism (Integral multiples of major lattice planes match across the interface) [16] can be invoked to explain the experimental observation. Therefore, with the introduction of an extra layer of Au (1-11) in the Au NP (indicated by the yellow arrow in Fig. 2c) oriented growth of Ag NPs can be realized.

Figure S3 shows another HAADF image and the corresponding Fourier filtered image to highlight the visibility of the interfacial dislocations in the two epitaxially grown Au NPs.

The epitaxially grown Au NPs are highly faceted with predominantly {111} facets and some {001} facets. Many HAADF images (e.g., Fig. 2a and 2c) seem to demonstrate that the Au NPs grew partially into the ZnO NW {10-10} facets and the close-packed Au{111} surfaces grew on top of the semi-polar ZnO{-1101} while the Au{001} surfaces also grew with a fixed orientational relationship with respect to the semi-polar ZnO{-110-1}. The exposed facets of the Au NPs are influenced by the nature of the hetero-epitaxy, especially for smaller Au NPs. The in-growth or entrenchment of the Au NPs requires modification of the original ZnO{10-10} nanoscale facets with a significant amount of the diffusion of Zn/O species. The ZnO also seemed to partially encapsulate (indicated by the yellow arrows in Fig. 2a) the Au NPs, implying a plausible strong metal support interaction (SMSI). The SMSI has rarely been observed in supported gold catalysts. Yin et al[17], however, found that during a high temperature treatment Au NPs inside a SiO_2 matrix could be encapsulated, presumably due to the crystallization of the SiO_2 support instead of SMSI. Recently, Liu et al[18] reported the observation of oxidative SMSI in their Au/ZnO-nanorod catalysts which are very similar to our Au/ZnO-NWs. They found that with O_2 treatment the Au NPs were fully encapsulated by ZnO species and that the Au NPs seemed to grow on pillars of ZnO species. Under H_2 treatment, they found that some Au NPs demonstrated feasible epitaxy and sunk into the ZnO support. Our repeated *ex situ* and *in situ* experiments with different treatment temperatures and conditions, however, never showed complete encapsulation of the Au NPs by the ZnO species. Figure 2d shows a bright-field phase contrast STEM image obtained simultaneously as that of Fig. 2c. Such images are useful for detecting surface layers of light materials. The highly faceted Au NP is partially embedded into the ZnO {10-10} nanofacets but the exposed Au surfaces are atomically clean[20].

The entrenchment of the Au NPs and the creation of Au{111}/ZnO{10-11} interfaces during the calcination treatment resulted in anchoring of the Au NPs by epitaxial growth. Although such crystal growth into the substrate is rare in metal/metal oxide systems similar observations has been reported in metal/semiconductor systems and such epitaxial growth is designated as endotaxy[19]: The deposited material forms oriented crystals that grow into the support material. Endotaxy mechanism has been utilized to grow embedded metal nanostructures for specific applications[19]. The detailed mechanisms of the endotaxial growth of noble metal NPs into metal oxide supports and the specific growth processes of noble metal NPs on the various ZnO nanofacets will be reported separately.

Epitaxy occurs in such a way that the total energy of the system, including the metal-substrate, metal-environment, and substrate-environment interfaces, is minimal. Thus the endotaxial Au NPs bind strongly to the surfaces of the ZnO NWs and should be more resistant to PMC processes even at elevated temperatures. The Au NPs are, however, still susceptible to sintering due to the Oswald ripening process. The hetero-epitaxy relationship did not change even after prolonged calcination at 600°C as shown in Fig. S4. The observed slow growth of the Au NPs at higher calcination temperatures is most probably due to Oswald ripening. The endotaxy of the Au NPs should alleviate their sintering by the Oswald ripening process as well.

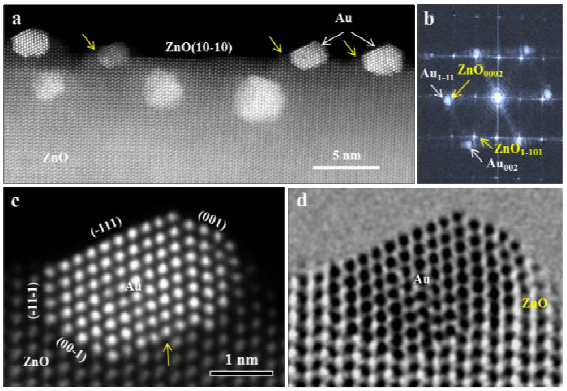

Figure 2. HAADF image (a) shows epitaxial growth of Au NPs into the ZnO {10-10} nanofacets. The Au NPs expose similar facets and are aligned. The ZnO NW was oriented to the ZnO [1-210] zone axis. The diffractogram (b) clearly shows the between the epitaxially grown Au NPs and the ZnO NW: Au[110](002)||ZnO[1-210](1-101). Atomic resolution HAADF image (c) shows the exposed nanofacets of the Au NP, the Au/ZnO interface structure and an interfacial misfit disloaction (indicated by the yellow arrow). Bright-field STEM image (d) shows the atomically clean Au nanofacets and the embedding of the Au NP into the ZnO.

It has been reported that Pt (Pd) NPs deposited on ZnO and under gas treatment can form PtZn (PdZn) alloys.[21] The formation of such alloy NPs can generally enhance the thermal stability of these NPs[22] and Au-M alloys have been adopted to improve the thermal stability of supported Au catalysts.[23] Both XRD data (Fig. S4) and atomic resolution HAADF images did not reveal the formation of any Au-Zn alloy phases even when the Au loading level was increased up to 5 wt% and the calcination temperature was increased to 600 °C. The XRD pattern showed that the ZnO NWs possess a wurtzite structure and that the Au NPs possess a standard face cantered cubic structure. Therefore, the synthesized Au/ZnO catalysts after calcinations up to 600 °C did not contain any Au-Zn alloy phases.

The size distribution of Au NPs affects their catalytic activity dramatically, especially for the CO oxidation reaction.[8a] We therefore chose CO oxidation as a probe reaction to evaluate the stability of the Au/ZnO catalyst systems. As shown in Figure 3a, for catalysts calcined at 200 °C, the Au/ZnO-P200 exhibited a higher activity than that of the Au/ZnO-NW200 primarily attributable to the size differences of the supported Au NPs (1.8 nm for powder-supported Au vs 2.4 nm for NW-supported NPs). When the supported Au NPs grew bigger after being calcined at 600°C the activity of both catalysts dropped. However, the two catalysts behaved very differently. If we use the T_{50} (the temperature for 50% CO conversion) as a measure of a catalyst's performance then the Au/ZnO-NW600 only increased by 70 °C while that of the Au/ZnO-P600 increased by about 300 °C, reflecting a significant sintering of the Au NPs in the Au/ZnO-P600 catalyst.

The specific reaction rate is a good indicator of the performance of a catalyst. Figure 3b shows that the Au/ZnO-P200 provided the highest activity for CO oxidation at 100 °C with a specific rate of 2.09 mol_{co} g_{Au}^{-1} h^{-1} but dramatically decreased to 0.52 and 0.062 mol_{co} g_{Au}^{-1} h^{-1}

(about 4 and 34 times of drop in activity) when the catalyst was calcined at 400°C and 600°C, respectively. In contrast, the Au/ZnO-NW catalyst only decreased 1.6 and 7 times when the catalyst was calcined at 400 and 600°C, respectively. These activity test results clearly demonstrated that the epitaxial growth of Au NPs into the ZnO NWs stabilized their movement during the high temperature calcination and the CO oxidation reaction. On the other hand, the ZnO powder-supported Au NPs sintered significantly during the high temperature calcination treatment. The reason for this significant sintering may be caused by the PMC process of the non-epitaxially grown Au NPs or the change of the surface structure of the ZnO powders. Figure 3c shows a long-term test of the two catalysts for CO oxidation at 150°C. After almost 20 hours the CO conversion of the ZnO NW-based catalyst Au/ZnO-NW400 only decreased about 10% (from ~ 83% to ~73%) and almost stabilized. On the other hand, the ZnO powder-based catalyst Au/ZnO-P400 decreased by more than 30% during the same testing period.

In conclusion, hetero-epitaxial growth of Au NPs into ZnO NWs has been successfully accomplished. The anchoring of Au NPs due to strong metal-support interaction has been demonstrated. The synthesized Au/ZnO-NW catalysts showed high activity for CO oxidation at moderate temperatures and resistant to sintering for calcination temperatures as high as 600°C. The approach to anchoring metal NPs by hetero-epitaxy is general and should provide new routes for developing stable, supported metal catalysts, especially supported Au NP catalysts, for broad applications in heterogeneous catalysis.

Acknowledgements

This work was funded by the start-up fund of the College of Liberal Arts and Sciences of Arizona State University and the Chinese Scholarship Council (CSC). The authors acknowledge the use of facilities in the John M. Cowley Center for High Resolution Electron Microscopy at Arizona State University.

Notes and references

1. (a)M. Haruta, N. Yamada, T. Kobayashi and S. Iijima, *J. Catal.*, 1989, **115**, 301; (b)M. Haruta, *Faraday Discuss.*, 2011, **152**, 11.
2. E. Roduner, *Chem. Soc. Rev.*, 2006, **35**, 583.
3. R. Ouyang, J.X. Liu and W.X. Li, *J. Am. Chem. Soc.*, 2013, **135**, 1760.
4.(a)C. R. Henry, *Surf. Sci. Rep.*, 1998, **31**, 231; (b)M. Bäumer and H.-J. Freund, *Prog. Surf. Sci.*, 1999, **61**, 127; (c)P. J. F. Harris, *Int. Mater. Rev.*, 1995, **40**, 97; (d)P. Wynblatt and N. A. Gjostein, *Prog. Solid State Chem.*, 1975, **9**, 21; (e)C. G. Granqvist and R. A. Buhrman, *Appl. Phys. Lett.*, 1975, **27**, 693.
5. J. Liu, *ChemCatChem*, 2011, **3**, 934.
6. (a)J. Liu, J. Wang and L. Allard, *Microsc. microanal.*, 2008, **14**, 262; (b)J. Liu, *Microsc. microanal.*, 2007, **13**, 544; (c)H. Liu and J. Liu, *Microsc. microanal.*, 2010, **16**, 1206; (d)J. X. Liu, Y. A. Song, B. T. Qiao, Y. D. Huang and J. Y. Liu, *Microsc. microanal.*, 2013, **19**, 1718; (e)J. X. Liu, Y. D. Huang and J. Y. Liu, *Microsc. microanal.*, 2014, **20**, 1986.
7. (a)N. Ta, J. J. Liu, S. Chenna, P. A. Crozier, Y. Li, A. Chen and W. Shen, *J. Am. Chem. Soc.*, 2012, **134**, 20585; (b)W. Z. Li, L. Kovarik, D. Mei, J. Liu, Y. Wang and C. H. Peden, *Nat. Commun.*, 2013, **4**, 2481; (c)J. Wang, A. H. Lu, M. Li, W. Zhang, Y. S. Chen, D. X. Tian &W.-C. Li, *ACS Nano*, 2013, **7**, 4902; (d)J. A. Enterkin, K. R. Poeppelmeier & L. D. Marks, *Nano Lett.*, 2011, **11**, 993.

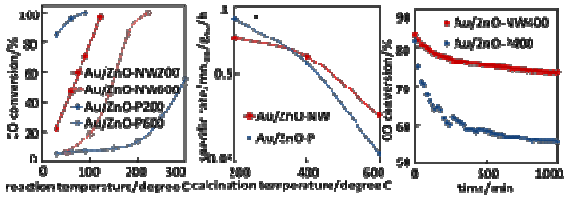

Figure 3. (a) CO conversion as a function of temperature over Au/ZnO-NW (red) and Au/ZnO-P (blue) with different calcination temperatures; (b) the specific rate of CO conversion at 100°C as a function of calcination temperature; (c) the stability test of Au/ZnO-NW400 and Au/ZnO-P400 catalyst for CO oxidation at 150°C. Reaction condition: CO: O2: He = 1: 1: 98, GHSV = 40,000mlg $^{-1}_{cat}$h $^{-1}$

8. (a)G. C. Bond and D. T. Thompson, *Catal. Rev.-Sci. Eng.*, 1999, **41**, 319; (b)M. Haruta, *CATTECH*, 2002, **6**, 102.
9.F. Yang, M.S. Chen, D.W. Goodman, *J.Phys.Chem.C*, 2008, **113**, 254.
10.(a)G. Y. Wang, W. X. Zhang, H. L. Lian, D. Z. Jiang and T. H. Wu, *Appl. Catal. A-Gen.*, 2003, **239**, 1; (b)T. Akita, P. Lu, S. Ichikawa, K. Tanaka and M. Haruta, *Surf. Interface Anal.*, 2001, **31**, 73.
11.G. C. Bond, C. Louis and D. T. Thompson, *Catalysis by Gold*, Imperial College Press, London, 2006.
12.C.W. Corti, R.J. Holliday & D.T. Thompson, *Top.Catal.*, 2007, **44**, 331.
13.(a)S. E. Golunski, *Platin. Met. Rev.*, 2007, **51**, 162-162; (b)T. Risse, S. Shaikhutdinov, N. Nilius, M. Sterrer and H. J. Freund, *Accounts Chem. Res.*, 2008, **41**, 949.
14.Z. W. Pan, Z. R. Dai and Z. L. Wang, *Science*, 2001, **291**, 91947.
15.(a) A. A. Herzing, C. J. Kiely, A. F. Carley, P. Landon and G. J. Hutchings, *Science*, 2008, **321**, 1331; (b) R. Zanella and C. Louis, *Catal. Today*, 2005, **107–108**, 768.
16. (a) J. Narayan and B. C. Larson, *J. Appl. Phys.*, 2003, **93**, 278; (b) S. Ramachandran, A. Chugh, A. Tiwari and J. Narayan, *J. Cryst. Growth*, 2006, **291**, 212; (c) A. Chugh, S. Ramachandran, A. Tiwari and J. Narayan, *J. Electron. Mater.*, 2006, **35**, 840.
17. H. F. Yin, Z. Ma, H. G. Zhu, M. F. Chi and S. Dai, *Appl. Catal. A-Gen.*, 2010, **386**,147.
18. X. Y. Liu, M. H. Liu, Y. C. Luo, C. Y. Mou, S. D. Lin, H. K. Cheng, J. M. Chen, J. F. Lee and T. S. Lin, *J. Am. Chem. Soc.*, 2012, **134**,10251.
19.(a) I. Bonev, *Acta. Crystallogr.*,1972, **A28**, 508.; (b) T. George and R. W. Fathauer, *Appl. Phys. Lett*., 1991, **59**, 3249.; (c) Z. He, D. J. Smith and P. A. Bennett, *Phys. Rev. Lett*., 2004, **93**, 256102.; (d) R.R. Juluri, A. Rath, A. Ghosh & P.V. Satyam, *J. Phys. Chem. C*, 2013, **117**, 13245.
20. Note: During TEM observations, high doses of electron beam can cause electron beam induced encapsulation of Au NPs and pillar-like growth of ZnO species. All the images reported in this communication were obtained with moderate electron beam irradiation to avoid electron beam effects.
21.(a) S. T. Liu, K. Takahashi, K. Fuchigami and K. Uematsu, *Appl. Catal. A-Gen.*, 2006, **299**, 58; (b) F. Ammari, *J. Catal.*, 2004, **221**, 32.
22.T. Chookajorn, H.A. Murdoch & C.A. Schuh, *Science*, 2012, **337**, 951.
23.(a) X. Liu, A. Wang, X. Yang, T. Zhang, C. Y. Mou, D. S. Su and J. Li, *Chem. Mat.*, 2009, **21**, 410; (b) X. Liu, A. Wang, X. Wang, C. Y. Mou and T. Zhang, *Chem. Commun.*, 2008, 3187.

